

## Dissipation of Currents in Ionized Media

O. BUNEMAN\*

Stanford University, Stanford, California

(Received February 6, 1959)

The destruction of electron drifts by instabilities is analyzed. The fastest stable drift is calculated (drift energy  $0.9kT$ ) and the energy of a faster drift is found to be dissipated into instabilities within, typically, 30 plasma periods. The growth of a local disturbance in this process is shown to take place without effective propagation. The "turbulent" flow pattern created, eventually, under nonlinear conditions is calculated numerically, demonstrating the tendency towards randomization of the initial drift energy. The effect stops "runaway" in about 100 plasma periods after which there is "heating" by "collective collisions" instead.

### I. INTRODUCTION

THIS paper describes how directed electron energy is dissipated in a plasma into random energy by "collective collisions" with the ions, i.e., collision in bunches. A mechanism for the buildup of bunches from small fluctuations was described briefly by the author<sup>1</sup> and it was estimated that the initial electron drift would thus be destroyed within some tens of plasma periods.

The sequence of events will be analyzed in detail here. The range of conditions under which the mechanism occurs is delineated. "Landau damping," due to a spread of velocities superimposed on the drift, prevents it when the drift energy falls below  $0.9kT$ . But for faster drifts the initial random energy distribution, residing partly in plasma oscillations, acts as a trigger to exponential buildup of fluctuations. Their energy reaches the level of the initial drift energy within about 30 plasma periods in typical situations.

If the buildup is excited locally, the fluctuations grow, spread and drift downstream but fail to get clear of the original source (see Fig. 4). Only by imparting to the ions a drift in the same direction as that of the electrons could the mechanism be used for controlled amplification.

If the initial excitation is planar (unidirectional plasma waves), the nonlinear equations describing the resulting high-level fluctuations can be programmed into a computer. The calculated electron flow pattern (Fig. 5) shows the transition from order to chaos by multi-stream formation and a kind of turbulence. There are signs of high-energy randomness and the ions, too, appear to be working up towards a clash (Fig. 6). This would bear thermonuclear fruits.

When the drift is created gradually by an applied field exceeding the runaway threshold  $\pi e^2 N/kT$ , instabilities catch up with the drift in about  $10^2$  plasma periods. The field then increases the energy of random streaming, i.e., it "heats" the plasma, keeping the drift energy just below the correspondingly rising  $kT$ . The

rapid dissipation by these "collective collisions" results in a high resistivity.

### II. TWO-STREAM INSTABILITY

We begin the analysis by putting on record the formulas governing the two-stream growth mechanism (see Pierce,<sup>2</sup> and references given therein). The field which originally imparted the drift to the electrons is supposed to have been taken off again, leaving only a fluctuation field  $\mathbf{E}$ . This causes velocities  $e\mathbf{E}/i\omega M$  of the ions (initially at rest), in the small signal approximation. The ion current density is then  $e^2 N \mathbf{E}/i\omega M$  and its negative divergence gives the rate of change of the ion charge density. Therefore the ion charge density fluctuations are  $(e^2 N/\omega^2 M)\nabla \cdot \mathbf{E}$ .

The electrons move, initially, with velocity  $\mathbf{u}$  and the frequency with which they encounter the fluctuations is Doppler-shifted by  $\boldsymbol{\beta} \cdot \mathbf{u}$ . Here  $\boldsymbol{\beta}$  is the wave-number vector of the fluctuations which we take to be Fourier-analyzed in space: the space-time variation is like  $\exp(i\omega t - i\boldsymbol{\beta} \cdot \mathbf{r})$  with real  $\boldsymbol{\beta}$  but possibly complex  $\omega$ . The electron velocities are, then,  $-e\mathbf{E}/i(\omega - \boldsymbol{\beta} \cdot \mathbf{u})m$  and their charge density fluctuations  $[e^2 N/(\omega - \boldsymbol{\beta} \cdot \mathbf{u})^2 m]\nabla \cdot \mathbf{E}$ . Substituting the two charge density fluctuations into Poisson's equation for  $\nabla \cdot \mathbf{E}$ , we get the dispersion formula:

$$\omega_{pi}^2/\omega^2 + \omega_{pe}^2/(\omega - \boldsymbol{\beta} \cdot \mathbf{u})^2 = 1, \quad (1)$$

where  $\omega_{pi}$  and  $\omega_{pe}$  are the ion and electron plasma frequencies.

The complex solutions  $\omega = \omega_r \pm i\alpha$  of the dispersion formula are plotted against  $\boldsymbol{\beta} \cdot \mathbf{u}$  in Fig. 1. Tables are

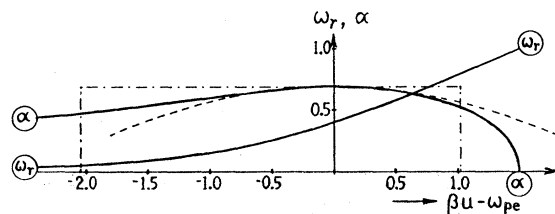


FIG. 1. Dispersion relation. Real part ( $\omega_r$ ) and imaginary part ( $\alpha$ ) of  $\omega$  versus  $\beta u - \omega_{pe}$ . Horizontal and vertical scales in units of  $(\omega_{pi}^2 \omega_{pe})^{1/2}$ .

<sup>2</sup> J. R. Pierce, *Traveling Wave Tubes* (D. Van Nostrand Company, Inc., New York, 1950), Chap. 2.

\* Work carried out at Stanford Electronics Laboratories, Stanford University under Air Force Contract while on academic leave from Cambridge, England. Author now at Peterhouse, Cambridge.

<sup>1</sup> O. Buneman, *Phys. Rev. Lett.* 1, 8 (1958).

given in reference 2. The exact formula  $\mathfrak{B} \cdot \mathbf{u} = \omega + \omega_{pe}$   $(1 - \omega_{pe}^2/\omega^2)^{-\frac{1}{2}}$  was replaced by the approximation

$$\mathfrak{B} \cdot \mathbf{u} = \omega_{pe} + \omega + \omega_{pe}\omega_{pe}^2/2\omega^2 \quad (2)$$

in the calculations.  $\mathfrak{B} \cdot \mathbf{u}$  is real for all  $\omega$  of the form  $(\omega_{pe}\omega_{pe}^2 \cos\theta)^{\frac{1}{2}}e^{i\theta}$ . At  $\theta = -\pi/3$  the growth rate  $\alpha$  maximizes to  $\alpha_m = \omega_{pe}(m/2M)^{\frac{1}{2}}3^{\frac{1}{2}}/2 (= 0.0562\omega_{pe}$  for  $H$ ), and  $\mathfrak{B} \cdot \mathbf{u} = \omega_{pe}$  at that point. But there is a range of about  $3(\omega_{pe}\omega_{pe}^2)^{\frac{1}{2}}$  ( $\sim \frac{1}{4}\omega_{pe}$  for  $H$ ) in  $\mathfrak{B} \cdot \mathbf{u}$  over which the growth rate is still quite close to its maximum.

Only the component of  $\mathfrak{B}$  in the direction of  $\mathbf{u}$  matters, or only the component of  $\mathbf{u}$  in the direction of  $\mathfrak{B}$ . There is no transverse dispersion. From (2) it follows that

$$d(\mathfrak{B} \cdot \mathbf{u})/d\omega = 1 - \omega_{pe}\omega_{pe}^2/\omega^3, \quad = 3 \quad \text{for } \theta = -\pi/3, \\ \alpha = \max, \quad (3)$$

so that the group velocity is  $\frac{1}{3}\mathbf{u}$  (see also Sec. VII). For future reference, we also put on record:

$$d^2(\mathfrak{B} \cdot \mathbf{u})/d\omega^2 = 3\omega_{pe}\omega_{pe}^2/\omega^4, \quad = -6/\omega \\ \text{for } \theta = \pi/3. \quad (4)$$

The (complex) *phase* velocity is quite small compared with  $u$ . This is related to the following crude picture of the mechanism. The electrons form a beam traversing a traveling-wave tube (see, for instance, Pierce<sup>2</sup>) formed by the ions: a slow electron plasma wave of velocity  $u - \omega_{pe}/\beta$  interacts with the wave of velocity  $\omega_{pe}/\beta$  which the ions, taking the place of a "slow wave structure," are capable of carrying.

### III. SCALES; JUSTIFICATION OF IDEALIZATIONS

Our calculation has ignored boundaries, initial ion and electron temperatures, collisions and relativistic effects. In justification, we consider the following significant lengths, arranged in ascending order of magnitude:

- (a)  $r_0 = e^2/mc^2 = 2.83 \times 10^{-13}$  cm, classical electron radius;
- (b)  $l = N^{-\frac{1}{3}}$ , mesh size if ions, or electrons, were arranged in cubic lattice;
- (c)  $\lambda_D = (kT/4\pi e^2 N)^{\frac{1}{2}}$ , Debye length;
- (d)  $L = 2\pi/\beta = 2\pi u/\omega_{pe}$ , preferentially growing space period of fluctuations, also distance traversed by electrons in one plasma period;
- (e)  $\lambda_p = 2\pi c/\omega_{pe} = 2\pi(mc^2/4\pi e^2 N)^{\frac{1}{2}} = (\pi l^3/r_0)^{\frac{1}{2}}$ , free-space wavelength of electromagnetic radiation at plasma frequency

(Gaussian units—replace  $4\pi e^2$  by  $e^2/\epsilon_0$  for *mks* units).

These lengths can be related to certain energies after introducing the following significant quantity:

$$W = e^2/l = mc^2 r_0/l = 1.44 \times 10^{-7} l^{-1} \text{ electron volt cm,} \\ \text{Coulomb energy of electron due to its} \\ \text{closest neighbor in cubic lattice.} \quad (6)$$

The four lengths (b) to (e) stand in the following

proportions:

$$\lambda_p : L : 2\pi\lambda_D : l = (mc^2)^{\frac{1}{2}} : (mu^2)^{\frac{1}{2}} : (kT)^{\frac{1}{2}} : (W/\pi)^{\frac{1}{2}}. \quad (7)$$

The ratio between the extremes,  $\lambda_p : l$ , equals  $(\pi l/r_0)^{\frac{1}{2}}$  and is proportional to  $N^{-1/6}$ . It is therefore not very sensitive to changes of conditions. For  $N = 10^{16}$  per cc one gets a ratio  $10^4$ , and this value we shall take as representative. In experiments connected with thermonuclear research we might be interested in imparting 250 electron-volt drift energy to the electrons ( $mu^2 = 10^{-3}mc^2$ ), in a plasma with initial temperature  $kT = 5$  electron volts ( $= 10^{-5}mc^2$ ). This would lead to the typical proportions:

$$\lambda_p : L : 2\pi\lambda_D : l = 10\,000 : 300 : 30 : 1. \quad (8)$$

Changing the numbers on the right by factors 3 either way will cover a wide variety of laboratory setups.

In astronomical applications the numbers would be spaced more widely. One has  $\lambda_p : l = 10^6$  when  $N = 10^8$  per cc. Temperatures would often be higher, although in interstellar space they might be down to  $kT = 10^{-6}mc^2$ , giving  $\lambda_p : 2\pi\lambda_D = 1000$ . The drift energies will vary from application to application and the order of  $L$  and  $2\pi\lambda_D$  might be reversed.

The absolute value of  $l$  ranges from  $10^{-5}$  cm in the laboratory to 1 cm in space, while  $\lambda_p$  goes from 1 mm to 30 km. In all cases  $L$ , the "grain size" of amplified fluctuations, is small compared with normal plasma dimensions. We may ignore boundaries. Specifically, we imply no assumptions regarding longitudinal terminations (in the direction of  $\mathbf{u}$ ): no "feedback" is needed. The model is *not* an electron beam injected into a stationary bed of ions from one end, but a uniform extended plasma in which all electrons are given the velocity  $\mathbf{u}$  by the application of a short external electric pulse. The plasma may be unending (toroidal) or finite but long compared with  $L$ .

The factor  $\sim 30$  between  $\lambda_p$  and  $L$ , i.e., between  $c$  and  $u$ , permits nonrelativistic treatment of the problem and neglect of self-magnetic fields. Electrostatics may be used and  $\mathbf{E}$ , the ion velocities, as well as the electron velocity perturbations, all have the direction of  $\mathfrak{B}$ . An applied magnetic field along a common axis of  $\mathbf{u}$  and  $\mathfrak{B}$  would have no effect. But other orientations have not yet been analyzed.

The factor 300 between  $L$  and  $l$  permits treatment of ions and electrons as continuous interpenetrating fluids. It also justifies neglect of close collisions. The target area is  $\sigma = \pi r_1^2$  where  $r_1$  is the radius at which Coulomb energy  $e^2/r_1 (= Wl/r_1)$  and drift energy  $\frac{1}{2} mu^2$  are equal. Hence  $r_1 = 2lW/mu^2 = 2\pi l(l/L)^2$ . We deduce the mean free path between collisions:

$$1/N\sigma = l^3/\pi(2\pi l^3 L^{-2})^2 = \frac{1}{4} L(L/\pi l)^3, \quad (9)$$

a quarter million times our scale of  $L$ .

We measure times in electron plasma periods ( $10^{-11}$  sec at  $N = 10^{14}$  per cc, proportional to  $N^{-\frac{1}{2}}$ ). Important events take place in a few tens of these:  $1/\alpha_m = e$ -folding time  $= 2.8 \times 2\pi/\omega_{pe}$  for  $H$ .

IV. INITIAL TEMPERATURE

Growth of fluctuations was calculated in Sec. II for an initially cold ion plasma traversed by a cold electron stream (but *some* noise was implied, to trigger off the growth). The closeness of  $L$  and  $2\pi\lambda_D$  in (8), i.e., the closeness of  $mu^2$  and  $kT$ , might make it difficult to justify the neglect of an initial temperature in applications not too different from those quoted as "typical." Indeed, one might be interested in situations where  $mu^2$  is less than  $kT$ , i.e., where the drift consists only of a slight bias in the thermal distribution.

Oscillations of an electron plasma which does not drift are known to suffer "Landau<sup>3</sup> damping" when the wave velocity decreases down to a few  $(kT/m)^{1/2}$  or less. Will such damping compete against the calculated growth, and at what temperature, or at what drift will the two balance?

Let  $f(\Delta u)du$  be the fraction of electrons whose velocity deviation from the mean,  $\bar{u}$ , lies within an interval  $du$  about  $\Delta u$ , i.e.,

$$f(\Delta u) = (2\pi kT/m)^{-1/2} \exp[-\frac{1}{2}m(\Delta u)^2/kT] \quad (10)$$

for a Maxwellian distribution. We only consider components of the vector  $\mathbf{u}$  in one direction, that of  $\beta$ , and we suppress, in this section, any suffix which might indicate that only this component is meant. Using the arguments of Sec. II separately for each velocity group of electrons traveling with velocity  $u = \bar{u} + \Delta u$ , we obtain the electron contribution to the left-hand side of a modified dispersion formula similar to (1):

$$\omega_{pe}^2 \int f(u - \bar{u}) du / (\omega - \beta u)^2.$$

Similarly, an ion velocity spread, characterized by the distribution function  $F(u)$ , gives a contribution  $\omega_{pi}^2 \int F(u) du / (\omega - \beta u)^2$  since here the mean is zero. Altogether, we get the dispersion formula:

$$\frac{\omega_{pe}^2}{\beta^2} \int \frac{f(u - \bar{u}) + (m/M)F(u)}{(w - u)^2} du = 1, \quad (11)$$

where  $w$  is the complex wave velocity,  $\omega/\beta$ . The imaginary part should be negative for amplification. An integration by parts yields

$$\int \frac{f'(u - \bar{u}) + (m/M)F'(u)}{u - w} du = \beta^2 / \omega_{pe}^2. \quad (12)$$

We insert the derivative of the function given by (10) and the similar function  $F(u)$  with the same temperature but, of course, the ion mass  $M$  in place of  $m$ . We also multiply (12) by  $kT/m$  and obtain

$$g\left(\frac{w}{(2kT/M)^{1/2}}\right) + g\left(\frac{w - \bar{u}}{(2kT/m)^{1/2}}\right) = \lambda_D^2 \beta^2, \quad (13)$$

<sup>3</sup> L. J. Landau, J. Phys. U.S.S.R. 10, 25 (1946).

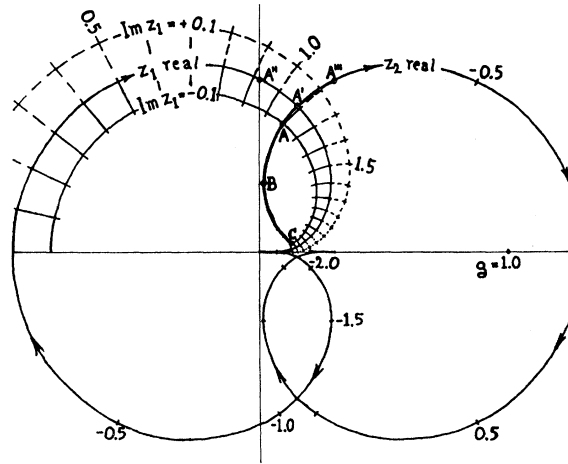


FIG. 2. Contour representation of  $g(z_1)$  and  $\lambda_D^2 \beta^2 - g(z_2)$  with  $\lambda_D^2 \beta^2 = 0.3$ . Contours for positive imaginary  $z_1$  are shown broken.

where

$$g(z) = -\pi^{-1/2} \int_{-\infty}^{+\infty} \frac{q \exp(-q^2)}{q - z} dq. \quad (14)$$

Note that the same function  $g(z)$  occurs in the first term (due to the ions) and the second term (due to the electrons). Only the arguments are different in the two terms. On the right we have used the Debye length as given in (5c).

Landau damping has its physical cause in the "resonance" between the wave velocity and that of a particular electron group:  $w = u$  (see Bohm and Gross<sup>4</sup>). Mathematically, this manifests itself in the singularity  $q = z$  of the integrand in  $g(z)$  and the resulting failure of  $g(z)$  to become real as  $z$  (and hence the frequency) approaches the real axis:

$$g(z) = -i\pi^{1/2} z \exp(-z^2) - \lim_{Q \rightarrow \infty} \pi^{-1/2} \int_{-Q}^{+Q} \frac{q \exp(-q^2) - z \exp(-z^2)}{q - z} dq, \quad (15)$$

on subtracting off the singular part of the integral in (14). The sign of the imaginary part in the first term is due to having  $z$  below the real axis (growth, disappearing as  $z$  becomes real). The integral in (15) is non-singular at  $q = z$  and becomes real as  $z$  becomes real. (The limits have to be taken to infinity simultaneously.) It is, incidentally, an *even* function of  $z$  (change  $q$  to  $-q$ ).

In Fig. 2 a contour representation of  $g(z)$  is given for  $z$ -values on and close to the real axis. The lower half of the  $z$ -plane is mapped inside a heart-shaped region. The diagram was constructed using the fact that

$$\frac{1}{2} z^{-1} \exp(z^2) [g(z) + 1] = \frac{1}{2} \pi^{-1/2} \int \frac{\exp(z^2 - q^2)}{z - q} dq,$$

<sup>4</sup> D. Bohm and E. P. Gross, Phys. Rev. 75, 1851 and 1864 (1949).

which is an error function of ( $iz$ ). [Integrate the identity

$$\left(\frac{\partial}{\partial q} + \frac{\partial}{\partial z}\right) \frac{\exp(z^2 - q^2)}{z - q} = 2 \exp(z^2 - q^2),$$

first with respect to  $q$  from  $-\infty$  to  $+\infty$  and then with respect to  $z$ , giving

$$\frac{1}{2} z^{-1} \exp(z^2) [g(z) + 1] = \int^z \exp(z'^2) dz',$$

where the lower limit has to be taken zero for the real part of  $g(z)$ , known to be even; the integral is tabulated.<sup>5</sup>] The contour diagram shows that one can make  $g(z)$  real positive, and thereby solve (13) with a single species only, by taking  $z$  in the upper half plane which represents ("Landau") damping. [The continuation of  $g(z)$  across the real  $z$ -axis without changing the sign of the first term in (15) is justified by the Laplace transform theory.]

To solve (13) as it stands, we plot  $z$ -contours of  $g(z)$  and  $\lambda_D^2 \beta^2 - g(z)$  in the same complex plane (Fig. 2) and compare the two complex labels  $z_1$  and  $z_2$  where the two heart-shaped regions overlap. There can be no overlap unless  $\lambda_D^2 \beta^2$  is less than 0.570. This means that only fluctuations with wavelengths longer than  $8.32\lambda_D$  will grow. As wavelengths increase, so does the region of overlap: the two hearts come closer together. Eventually, there will be overlap near the two cusps. Here the moduli of  $z_1$  and  $z_2$  are large and the approximation  $g(z) \approx 1/2z^2$  becomes valid, yielding the zero-temperature dispersion formula (1).

If either  $|z_1|$  or  $|z_2|$  is large, one is forced into the vicinity of both cusps, and hence towards the zero-temperature approximation. We may therefore assume in the following that neither is large and, in particular, that the imaginary parts are both moderate. Now we have

$$z_1 = w(M/2kT)^{1/2}, \quad z_2 = (w - \bar{u})(m/2kT)^{1/2}, \quad (16)$$

say, and since  $\bar{u}$  is real,  $\text{Im}(z_1)$  is at least 43 times larger than  $\text{Im}(z_2)$ . This means that the latter is negligible and our choice of representative points in Fig. 2 is restricted to the curve for real  $z_2$ . If we aim at a definite growth rate, i.e., if we fix the imaginary part of  $z_1$ , we restrict ourselves to a contour such as  $ABC$ , and only at  $A$  and  $C$  can both relations (16) be met.

The real parts of  $z_1$  and  $z_2$  are always opposite in sign when they refer to the same point in our diagram. Let us take  $\text{Re}(z_1)$  positive and  $\text{Re}(z_2)$  negative, i.e., consider the upper half of Fig. 2. From (16) we obtain

$$\begin{aligned} \bar{u} &= z_1(2kT/M)^{1/2} - z_2(2kT/m)^{1/2} \\ &= \text{Re}(z_1)(2kT/M)^{1/2} + |\text{Re}(z_2)|(2kT/m)^{1/2}. \end{aligned} \quad (17)$$

The slowest drift therefore occurs at the matching point  $A$  and the drift can be made slower at the cost of growth rate, i.e., by reducing the imaginary part of  $z_1$ , until

<sup>5</sup> E. Jahnke and F. Emde, *Tables of Functions* (Dover Publications New York, 1945), fourth edition, p. 32.

the match occurs at  $A'$ . [This procedure lowers both  $|\text{Re}(z_2)|$  and  $\text{Re}(z_1)$ .] One can then reduce  $\bar{u}$  still further by going to longer wavelengths and bringing the hearts closer until the points  $A''$  and  $A'''$  coincide where  $z_1 = -z_2 = 0.926$  and hence

$$\bar{u}_{\text{min}} = 0.926(2kT/m)^{1/2} [1 + (m/M)^{1/2}]. \quad (18)$$

The slowest drift leading to (just disappearing) growth of very long wavelengths of fluctuations is given by (18). Putting it the other way, (18) gives the fastest stable drift. The critical drift energy per electron,  $\frac{1}{2} m\bar{u}^2$ , is  $0.86 [1 + (m/M)^{1/2}]^2 kT$ . This is  $0.90kT$  for hydrogen. (A similar result was communicated to the author by M. Rosenbluth.) In terms of current densities, we can say that anything in excess of  $eN(1.8kT/m)^{1/2}$  will lead to instability.

## V. INITIAL FLUCTUATION ENERGY

We return to the study of situations where the drift is many times  $(kT/m)^{1/2}$  and where the wavelength of the significant fluctuations is many times  $\lambda_D$ , as indicated by the typical proportions in (8). We wish to know from what level of fluctuation intensity the process of growth begins.

Our model is, again, that of a plasma in equilibrium in which the electrons are given a short electric impulse to make them drift, and that during the action of this impulse the relative energy distribution in the electron cloud is not disturbed significantly (see Sec. XIII). Now a plasma in equilibrium is not neutral. Its heat is distributed among the  $6N$  degrees of freedom of the electrons and ions as well as the "free" i.e., undamped, plasma oscillations.

To find out how many degrees of freedom are available in such undamped plasma oscillations, we require an estimate of the wavelengths for which there is no Landau damping. One might think that in a Maxwellian distribution, containing some electrons of arbitrarily high velocity, all waves will suffer Landau damping. This is not so since the continuous fluid model breaks down for velocity groups at a few times  $(kT/m)^{1/2}$ . Only one electron in 700 exceeds (or falls short of) the mean velocity by more than  $3(kT/m)^{1/2}$ , and among  $10^{15}$  electrons not a single one can be expected to exceed the mean by more than  $8(kT/m)^{1/2}$ . From about  $3(kT/m)^{1/2}$  up, corresponding to wavelengths longer than  $6\pi\lambda_D$  at plasma frequency, particles become too widely spaced to be held responsible for Landau damping. (See (8) for relation between  $2\pi\lambda_D$  and  $l$ , the spacing of *all* particles.) Note also that the contour for real  $z$  in Fig. 2 merges into the real axis between  $3(kT/m)^{1/2}$  and  $4(kT/m)^{1/2}$ , effectively, indicating practically zero Landau damping, if we may still accept the continuum theory in this range.

Let us, therefore, consider plasma oscillations with phase velocities exceeding  $3(kT/m)^{1/2}$  as "free" modes. This makes available all wave numbers less than  $1/3\lambda_D$ . On the other hand, wave numbers must be multiples of

$2\pi \text{ cm}^{-1}$  if we study a plasma occupying just a cubic volume of 1-cm side. In the space of the  $\beta$ -vectors we are thus filling a spherical volume, of radius  $1/3\lambda_D$ , with mesh points spaced  $2\pi$  apart in each direction (see Fig. 3). This gives  $(4\pi/3)(6\pi\lambda_D)^{-3}$  free oscillators. Each carries energy  $kT$  (kinetic energy+field energy).

When the drift has been created, the energy of oscillators in a certain section of the  $\beta$ -sphere will be amplified rapidly. Taking the  $\beta_1$ -axis in the direction of  $\mathbf{u}$ , we get a section of thickness  $\delta\beta_1 \approx 3\omega_{pe}(m/M)^{1/2}/u \approx \frac{1}{4}\omega_{pe}/u = \pi/2L$  for  $H$ . (See Fig. 3.) The section straddles the level  $\beta_1 = \omega_{pe}/u = 2\pi/L$ . From (8) we see that this is rather less than the radius  $1/3\lambda_D$ . The section is therefore a disk of radius  $1/3\lambda_D$  and thickness  $\delta\beta_1$ , having volume  $\pi\delta\beta_1/9\lambda_D^2$  and containing  $\delta\beta_1/72\pi^2\lambda_D^2$  meshpoints.

Each meshpoint stands for an oscillator carrying energy  $kT$ . The amplifiable energy is therefore  $(\delta\beta_1/18)kT/(2\pi\lambda_D)^2$  which, according to the proportions (7) equals  $(\delta\beta_1/18)mu^2/L^2$ . We are referring here to a unit volume of plasma and on comparing this energy with the drift energy imparted to a unit volume,  $\frac{1}{2}Nmu^2$ , we obtain:

$$\frac{\text{amplifiable fluctuation energy}}{\text{directed drift energy}} = \frac{\delta\beta_1 l^3}{9 L^2}. \quad (19)$$

This ratio no longer depends on the size of the volume of plasma considered. Surprisingly, it is also independent of temperature. For hydrogen ( $\delta\beta_1 \approx \pi/2L$ ) we get about one-sixth of  $(l/L)^3$  which would be one part in about 150 million for the typical case described by (8).

## VI. BUILDUP TIME

Since amplitudes have an  $e$ -folding time of about 2.8 plasma periods, energies will be  $e$ -folded in 1.4 plasma periods and just about doubled in one plasma period. In 27 plasma periods the initial fluctuation energy will

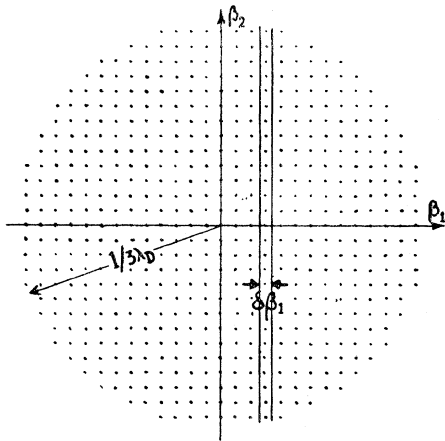


FIG. 3. Free plasma oscillators in  $\beta$  space. Outer boundary set by Landau damping. Section of thickness  $\delta\beta_1$  available for strong amplification.

therefore be amplified to the level of the directed drift energy, typically.

This estimate ignores the fact that the growth rate  $\alpha$  is not uniformly equal to  $\alpha_m$  over the entire band of width  $\delta\beta$ . (We suppress the suffix in this section.) In a more accurate calculation we consider an infinitesimal band of width  $d\beta$  and obtain from (19) that the ratio between fluctuation and drift energy becomes, after a time  $t$ ,

$$(\beta^3/9L^2)e^{2\alpha(\beta)t}d\beta = (2\pi/9)(l/L)^3\omega_{pe}^{-1}e^{2\alpha(\beta)t}d(\beta u). \quad (20)$$

We now integrate in (20) over a wide band of  $(\beta u)$  and approximate in the exponent by using a quadratic relation between  $\alpha$  and  $\beta$ , fitted to the actual relation at the point  $\beta u = \omega_{pe}$ ,  $\alpha = \alpha_m$  where most of the contribution to the integral originates ("method of steepest descent"). The data for obtaining the curvature of the  $\alpha, \beta$  graph (see Fig. 1) are given in (3) and (4) in that  $d^2\omega/d(\beta u)^2 = 2/9\omega$  at the maximum. Taking the real part, and using  $\alpha_m^2 = \frac{3}{4}|\omega|^2$  we get  $d^2\alpha/d(\beta u)^2 = -1/6\alpha_m$  at the maximum and hence the exponent in (20) becomes  $2\alpha_m t - (\beta u - \omega_{pe})^2 t / 6\alpha_m$  for our purposes. The integration now yields:

$$\frac{\text{fluctuation energy}}{\text{drift energy}} = \frac{2\pi}{9\omega_{pe}} \left(\frac{l}{L}\right)^3 \left(\frac{6\pi\alpha_m}{t}\right)^{1/2} e^{2\alpha_m t}. \quad (21)$$

Inserting the values  $\alpha_m = 0.0562\omega_{pe}$  appropriate to hydrogen, as well as  $L = 300l$  in accordance with (8), one finds that the ratio reaches unity when  $\omega_{pe}l/2\pi = 28.4$ , i.e., in 28.4 plasma periods.

We see that our first estimate was not far out. Moreover, since the square root of  $t$  in the denominator in (21) varies slowly, we can employ a straight-forward exponential law for the build-up of the fluctuation energy in the study of conditions (i.e.,  $l/L$  values) not too different from those taken as typical here: roughly, the energy doubles in one plasma period.

According to (5b) and (5d), or according to (6) and (7), the ratio  $L/l$  is proportional  $uN^{-1/6}$ . Hence the "buildup time," i.e., the time within which fluctuations are amplified to drift level, is increased above 28.4 plasma periods by  $1\frac{1}{2}$  plasma periods for every doubling of the drift energy above that assumed for (8). The time is reduced by  $\frac{1}{2}$  plasma period for every doubling of the plasma density. In terms of the ratio  $L/l$ , we can put

$$\begin{aligned} \text{buildup time (in plasma periods)} \\ \approx 28.4 + 3 \log_2(L/300l) \\ \approx 3.6 + 10 \log_{10}(L/l), \end{aligned} \quad (22)$$

provided  $L/l$  does not differ from 300 by a large factor.

The drift distance during buildup time is just  $L$  times the number given by (22). Since buildup takes place at the cost of drift energy, this distance is that within which the drift is destroyed, i.e., the electrons are stopped. The distance should be compared with the collision mean free path given by (9). While the latter goes up like  $(L/l)^3$ , the drift distance goes up only like

the logarithm to the base 2 of  $(L/l)^3$ . Even in partly ionized media the calculated buildup time, or drift stopping time, measured in tens of plasma periods only, is often short compared with the time between collisions with neutrals.

VII. GROWTH OF A LOCAL DISTURBANCE

In the last section we have assumed that the growth is triggered off by the random fluctuations that are present in every plasma. It was convenient to do this by means of a Fourier analysis in space. One would like a more direct picture, not in terms of a Fourier spectrum, how local nonuniformities of the plasma grow and spread under the two-stream mechanism.

Let us therefore put in a strictly localized perturbation at the origin  $(x, y, z) = (0, 0, 0)$ . We take  $\mathbf{u}$  along the  $x$  axis and describe the disturbance mathematically as the product of three delta-functions,  $\delta(x)\delta(y)\delta(z)$ . Since our dispersion law is in terms of Fourier components, we must Fourier-analyze each delta-function, for instance:

$$\delta(x) = (2\pi)^{-1} \int e^{-i\beta_1 x} d\beta_1. \tag{23}$$

Now we know that the dispersion formula does not involve  $\beta_2$  or  $\beta_3$ . Hence there is no dispersion or "dispersal" of the perturbation in the  $y$  and  $z$  directions. The perturbation remains confined transversely to  $\mathbf{u}$ , and we need only consider its development in the  $x$ -direction. Again, we suppress henceforth the suffix "1" of  $\beta_1$  in this section.

After time  $t$  the Fourier spectrum will have changed from that given by (23) to

$$f(x,t) = (2\pi)^{-1} \int e^{i[\omega(\beta)t - \beta x]} d\beta. \tag{24}$$

Here  $\omega(\beta)$  is that solution of the dispersion formula which represents growth: its contribution will overshadow those due to decaying or steadily oscillating modes. Again, we use the method of steepest descent<sup>6</sup> to evaluate the integral, in that we look for that (possibly complex) value of  $\beta$ , and the corresponding  $\omega$ , for which the exponent becomes stationary.

By differentiating the exponent, and equating to zero, we get

$$ut/x = d(\beta u)/d\omega = 1 - \omega_{pe} \omega_{pe}^2 / \omega^3, \tag{25}$$

[see (3)]. We solve for  $\omega$ ,

$$\omega = [\omega_{pe}^2 \omega_{pe} x / (ut - x)]^{1/3} e^{-i\pi/3}, \tag{26}$$

and substitute this value into formula (2) to give  $\beta u$ :

$$\beta u = \omega_{pe} + \frac{1}{2} \left[ \frac{\omega_{pe}^2}{x^2} \frac{\omega_{pe}}{(ut - x)} \right]^{1/3} (3x - ut) e^{-i\pi/3}. \tag{27}$$

Now we substitute in the exponent from (26) and (27), giving the value of the exponent where it is stationary with respect to changes of  $\beta$ :

stationary exponent  

$$= -i\omega_{pe}(x/ut) + \frac{3}{2} i e^{-i\pi/3} [\omega_{pe}^2 \omega_{pe} (ut - x)^2 x]^{1/3} / u. \tag{28}$$

In the further application of the method of steepest descent, we ought now to construct a quadratic approximation to the exponent (as a function of  $\beta$ ) in the vicinity of its stationary value, as we did in the previous section between Eqs. (20) and (21). The integration can then be carried out and the square root of the second derivative of the integrand with respect to  $\beta$  appears in the denominator of the result. This is rather a slowly varying function of  $x$  and  $t$  and we need not reproduce the details of the calculation here.

The dominant factor in the result of the integration is, of course, the stationary value of the exponential, for the exponent, as shown by (28), has a positive real part which grows like  $(ut - x)^{2/3} x^{1/3}$ . The logarithm of the amplitude is therefore proportional to this quantity (but for the weak dependences mentioned in the preceding paragraph), and we have plotted the quantity *versus*  $x$  for various  $t$  in Fig. 4.

As time progresses, we see, the disturbance is drawn out between its initial position and the position  $x = ut$  to which the electrons have advanced. While it spreads it grows in intensity everywhere. It never clears the origin. This means the mechanism can not be used for controlled amplification of signals injected at one place and taken out further down the line. Both ions and electrons would have to be made to drift in the same direction in an amplifier based on this principle, so that successive curves in Fig. 4 would be translated rightwards, always clearing the origin for the injection of further signals.

The maximum of  $(ut - x)^2 x$  occurs at  $x = \frac{1}{3} ut$  and the peak of the disturbance therefore travels with velocity  $\frac{1}{3} u$ , the "group velocity" calculated in Sec. II from Eq. (3). The growth rate at the peak is found, on substitution of  $x = \frac{1}{3} ut$  into (28), to be  $\alpha_m$ .

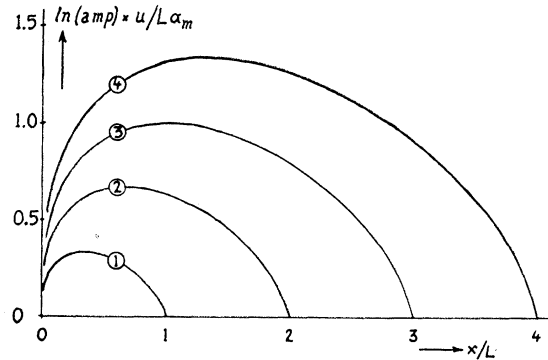


FIG. 4. Growth and spread of local disturbance. Logarithm of amplitude *versus* distance (downstream) from origin, at successive times: (1) at  $t = L/u$ , (2) at  $t = 2L/u$ , (3) at  $t = 3L/u$ , (4) at  $t = 4L/u$ .

<sup>6</sup> H. Jeffreys and B. S. Jeffreys, *Methods of Mathematical Physics* (Cambridge University Press, Cambridge, 1946), Chap. 17.04 p. 472.

A study of the imaginary part in formula (28) reveals that this differs by less than 1% from  $\omega_{pe}x/u$ , for hydrogen. Hence at all times the disturbance will exhibit ripples of periodicity  $L (= 2\pi u/\omega_{pe})$ .

### VIII. NONLINEARITY

So far, we have calculated growth of fluctuations by a linearized theory. During the last few plasma periods of the buildup, however, while most of the conversion of directed energy into fluctuation energy occurs, nonlinear effects are bound to become important. For instance, the drift velocity, hitherto treated as constant, must decrease as the fluctuations consume drift energy.

However, even in the absence of a mutual drift between ions and electrons, and even when ion motions are ignored altogether, nonlinear effects take place in the oscillations of a pure electron plasma when they are excited to a sufficiently high level. These effects were calculated by Sturrock.<sup>7</sup>

In the case of interaction between ions and electrons by the two-stream mechanism, nonlinearities will manifest themselves in the dynamics of the electrons in the first place. For the electron velocity perturbations, as well as their density perturbations, are larger than those of the ions: substitution of the maximum growth solution  $\omega = (\omega_{pe}^2 \omega_{pe}/2)^{1/2} \exp(-\frac{1}{2}i\pi)$ ,  $\mathfrak{z} \cdot \mathbf{u} = \omega_{pe}$  of the dispersion formula (2) into the expressions quoted for velocities and densities in the derivation of the formula leads to the following ratios:

$$\frac{\text{ion velocity}}{\text{electron velocity fluctuation}} \approx 2 \left( \frac{m}{2M} \right)^{1/2} = 0.0084 \quad \text{for H, (29)}$$

$$\frac{\text{ion density fluctuation}}{\text{electron density fluctuation}} \approx 2 \left( \frac{m}{2M} \right)^{1/2} = 0.13 \quad \text{for H. (30)}$$

In view of the importance of the dynamics of the electrons in connection with nonlinearities, it is convenient to visualize phenomena in a frame which travels with the mean electron velocity. The ions are then moving and nonlinearities in their dynamics may be ignored. They are merely a means of exciting electron plasma oscillations which take place at the Doppler-shifted frequency  $\omega_{pe} - \omega \approx \omega_{pe}$ . (Wave numbers  $\beta_1, \beta_2, \beta_3$  are not altered in a nonrelativistic transformation.) The ions are the "bow," the electrons the "string." However, this would not be the correct frame for describing the slowing down mentioned in the first paragraph of this section: since momentum is conserved, the energy balance must be drawn up in the center-of-gravity frame of ions and electrons: this is, more or less, the frame of the ions.

Applying the results of Sturrock's calculations for an electron plasma, we may conclude, perhaps, that non-

linearity will serve to restore isotropy of the Fourier spectrum (the tendency towards isotropy is the main effect of nonlinearity derived by Sturrock). The spectrum created by the growth mechanism from an initially isotropic spectrum in  $\mathfrak{z}$ -space (see Fig. 3), although still isotropic in the directions transverse to  $\mathbf{u}$  ( $\beta_2$  and  $\beta_3$ ), contracts to a narrow band in the longitudinal component  $\beta_1$ . Although growth is appreciable over a fairly wide band in  $\beta_1$  (about 25% of the mean  $\beta_1 = \omega_{pe}/u$ ), after the 28.4 plasma periods of buildup there is quite a noticeable selectivity effect: inserting the appropriate  $t = 10/\alpha_m$  into the parabolic approximation for the exponent  $2\alpha(\beta)t$  in (20), one finds the energy drops to half the peak value when  $\beta_1$  differs as little as 3.6% from  $\omega_{pe}/u$ .

The sharpness of this spectrum will be reduced again by nonlinearity. Eventually, isotropy should be restored and the drift energy distributed evenly among all the available plasma oscillators. However, the distribution may not be completely random: results obtained from the application of Fourier analysis to a nonlinear problem must be treated with caution. Correlations revealed by alternative methods (where such are available) may be missed.

### IX. ONE-DIMENSIONAL PHENOMENA

In his analysis of nonlinear plasma oscillations Sturrock finds that strictly one-dimensional spectra behave in a singular manner: there is, to the order to which the investigation is taken, no long-term ("secular") redistribution of energy among different Fourier components whose  $\mathfrak{z}$ -vectors all have the same direction. One wonders whether the spectra which have appeared in our work (the tips of all  $\mathfrak{z}$ -vectors lie in a plane  $\beta_1 = \text{constant}$ ) would exhibit similar peculiarities. Moreover, if we did start with a one-dimensional spectrum, narrowed down to a single  $\mathfrak{z}$ -vector by the selectivity of the amplification process, would nonlinearity fail to effect the return to randomness?

Fortunately, a more direct approach than Fourier analysis can be followed when the problem is one-dimensional. It explains the persistence of the spectrum and reveals the underlying correlations. It also shows that randomness is restored eventually, when amplitudes have grown sufficiently, within that one dimension.

The method consists of changing from the Eulerian description of the electron and ion fluids (recording velocities and densities as distributions in space and time) to the Lagrangian description (tracing histories of individual particles or groups of particles). Since there is uniformity in two of the three dimensions ( $y$  and  $z$ , say), we divide the plasma into a large number of very thin plane disks of ions and electrons and record their displacements,  $x$ , as functions of time and a parameter  $s$  which distinguishes the disks from each other.

The direction  $x$  need not coincide with that of the initial drift,  $\mathbf{u}$ . There may be a "sheared" component of the drift in the  $(y, z)$  planes of the disks. All we require

<sup>7</sup> P. A. Sturrock, Proc. Roy. Soc. London A242, 277 (1957).

is that this component should remain uniform, velocity perturbations being restricted to the  $x$  component. A uniform transverse drift within each disk can be ignored, both in the equations of motion and in the equations for the field.

The parameter  $s$  is conveniently chosen as the displacement of each disc from some fixed origin a long time ago, before perturbations of the uniform distribution had occurred. Then  $eNd_s$  is the charge per unit area of a disk associated with the interval  $ds$  of the parameter  $s$ . If  $E(0)$  is the field at  $x=0$  then, by Gauss' theorem,

$$E(x) = E(0) + 4\pi eN \left( \sum \int_{S_\nu(0)}^{S_\nu(x)} dS - \sum \int_{s_\nu(0)}^{s_\nu(x)} ds \right), \quad (31)$$

where capitals have been used to distinguish the ions from the electrons and where the integrations are over all those ranges of  $s$  and  $S$  from which disks originate that lie between 0 and  $x$  at time  $t$ . There may be several such ranges, in that the original order may not have been preserved: hence the sums. In terms of large numbers of disks, each of finite original thickness  $\delta s$ , the bracket can be understood as the number of ion disks, minus the number of electron disks in the interval between 0 and  $x$ , multiplied by  $\delta s$ .

To get  $E(0)$ , we calculate the potential drop between 0 and  $x=X$ . By (31), an ion disk contributes nothing to the field on its left and  $4\pi eNdS$  to the field on its right. To the potential drop it therefore contributes  $4\pi eN(X-x)dS$ . Similarly for the electrons, and hence the potential drop is

$$XE(0) + 4\pi eN \left( \sum \int_{S_\nu(0)}^{S_\nu(X)} (X-x)dS - \sum \int_{s_\nu(0)}^{s_\nu(X)} (X-x)ds \right). \quad (32)$$

If the potential drop is fixed by external conditions, then we can determine  $E(0)$  from (32) and hence evaluate the field anywhere with the aid of (31).

The expression (32) simplifies in two more or less complementary extreme cases, namely when the disturbance is localized and limited to the interior of the range between 0 and  $X$ , or when it is strictly periodic and  $X$  is identified with the period,  $L$ . In both cases the total ranges of  $S$  and  $s$  in the expression are equal to each other. In the first case because at the ends, 0 and  $X$ , conditions are unperturbed so that all the ions in the range are those which were there originally, i.e., those with  $0 < S < X$ , while the electrons originate from an  $s$ -range of equal length, but further up-stream. In the second case the ions must originate from an  $S$ -range, the electrons from an  $s$ -range, both exactly of length  $L$ .

In these situations we get cancellation of the sums of the integrals  $\int XdS$  and  $\int Xds$  while the integrals  $\int xdS$  and  $\int xds$  can be written as averages,  $\bar{x}(S,t)$  and  $\bar{x}(s,t)$ , multiplied by the total range,  $X$ . Dividing the potential drop by  $X$ , to give the mean field  $\bar{E}$  over the

range, we then obtain

$$E(0) = \bar{E} + 4\pi eN[\bar{x}(S,t) - \bar{x}(s,t)]. \quad (33)$$

In the bracket we have the difference between the average positions  $\bar{x}_i$  and  $\bar{x}_e$  of all the ions and all the electrons in the interval.

We substitute (33) into (31) and equate the field to  $(M/e)\ddot{x}_i$  and  $-(m/e)\ddot{x}_e$ . Dividing by  $4\pi eN$ , this leads to

$$\omega_{pi}^{-2}\ddot{x}_i = -\omega_{pe}^{-2}\ddot{x}_e = \bar{x}_i - \bar{x}_e + \sum \Delta S - \sum \Delta s + \bar{E}/4\pi eN. \quad (34)$$

Here  $\Delta S$  stands for  $S(x) - S(0)$  and  $\Delta s$  for  $s(x) - s(0)$ . The summation is over all the ranges that contribute disks in the interval. In terms of sets of discrete disks of standard finite initial thickness, the sums represent the fraction of disks in the interval between 0 and  $x$ , out of all those between 0 and  $X$ , multiplied by  $X$ .

The choice of an origin 0 for this "count" is to some extent arbitrary. In the application to a confined disturbance the only requirement is that 0, as well as the terminal  $X$ , should lie outside the disturbance. In the application to a periodic disturbance the only requirement is that 0 and  $X$  should be one period apart. We need not take the same 0 at all times but can let 0 follow a particular electron, say.

Equations (34) are rigorous and we proceed to regain from them the equation describing ordinary plasma oscillations. To this end, we cut out the external field  $\bar{E}$ , we make the ions infinitely heavy and stationary, so that  $x_i = S = \text{constant}$  and we also suppose that the electrons keep their original order. We get  $\bar{x}_i = \bar{S} = \frac{1}{2}X$  and if we take as origin for the count a specific electron disk, say that characterized by  $s=0$ , we get  $\Delta S = S(x) - S[x(0)] = x - x(0)$ . Also, since  $x(0)$  is not the permanent coordinate origin, we should write  $\bar{x}_e - x(0)$  in place of  $\bar{x}_e$ . Since the electrons keep their order, we have  $\Delta s = s = \text{constant}$  along an electron orbit. The equation of motion for the electrons then reduces to

$$-\omega_{pe}^{-2}\ddot{x} = \frac{1}{2}X + x - x(0) - [\bar{x} - x(0)] - s = \frac{1}{2}X + x - \bar{x} - s \quad (35)$$

omitting the subscript "e."

We note that  $\bar{s} = \frac{1}{2}X$  and hence that the average of all accelerations vanishes: the average moves with uniform drift. From this we deduce

$$-\omega_{pe}^{-2}(d^2/dt^2)(x - \bar{x} + \bar{s} - s) = x - \bar{x} + \bar{s} - s, \quad (36)$$

and hence

$$x - s = \bar{x} - \bar{s} + A_s \cos(\omega_{pe}t - \phi_s). \quad (37)$$

Relative to the drift, each layer performs strictly harmonic motion with no limitation of amplitude other than that arising from the condition that the order should be preserved. The latter condition is that  $\partial x/\partial s$  should always have the same sign, which becomes

$$(dA_s/ds)^2 + A_s^2(d\phi_s/ds)^2 < 1. \quad (38)$$

The linearity of (35) and (36) explains why Sturrock,<sup>7</sup> using Eulerian coordinates and Fourier analysis, obtained a singular behavior for one-dimensional spectra. Using Lagrange coordinates and avoiding Fourier analysis, the equations turn up in linear form. Whatever the spatial distribution of amplitudes and phases [subject only to condition (38)], the motion remains strictly periodic in time. There is no randomization and the motion is strongly "correlated": each pattern of disturbances is repeated strictly with period  $2\pi/\omega_{pe}$ . There are no secular changes.

One could now proceed to calculate small corrections to the strict solution (37) due to small-amplitude motion of the ions, employing linearization only in these corrections, wherever necessary. This leads back to equations like those obtained by the Eulerian method (which we employed in Sec. II), and to the dispersion formula (1). Thus one gains confidence that the theory is restricted to small amplitudes only as regards the ions, not as regards the electrons. For the latter we only have the restriction that there should be no overtaking, i.e., that (38) is satisfied.

If now we assume periodicity of the perturbations with period  $L$  in space, and if, in particular, the dependence upon  $s$  is simple harmonic, we must take the amplitudes  $A_s$  independent of  $s$  and  $\phi_s$  linear in  $s$ , as follows:

$$A_s = \text{constant}, \quad \phi_s = 2\pi s/L. \quad (39)$$

The condition (38) then leads to

$$|A_s| < L/2\pi = u/\omega_{pe}, \quad (40)$$

taking the period  $L$  to which the fluctuation spectrum narrows down. With the extreme displacement amplitude [equality rather than inequality in (40)] one obtains the velocity amplitude  $u$  by differentiation of (37). Hence the mean kinetic energy is  $\frac{1}{4}mu^2$  and the potential energy likewise: the entire initial drift has just been converted into fluctuation energy of the electrons when the level giving overtaking is reached (the energy stored in ion motion may be ignored compared with that of the electrons). Presumably, the perturbation method described above would exhibit a secular reduction of the drift, if carried out in full detail.

#### X. COMPUTATION OF LARGE-AMPLITUDE ONE-DIMENSIONAL PHENOMENA

We have outlined an analytic procedure which would take the calculation of transient buildup to the level of electron-overtaking, with only minor approximations. However, rather than following through this procedure, we have set up the Eqs. (34) for numerical integration: this enables one to go beyond the point of electron-overtaking.

Some of the information obtained by analysis was utilized in the computations. For instance, the fact that a definite space-period crystallizes out of linear buildup became an essential ingredient: the situation was even

idealized into the condition that the periodicity should be strict. It then persists, of course, throughout the nonlinear development of perturbations.

The periodicity allowed limitation of the number of ion disks and electron disks to be traced. 256 of each kind were taken in one period of length  $L$ . The evaluation of the accelerations given by (34) then amounted to a simple count of the disks between the disk to be accelerated and a fixed origin. Displacements were recorded only "modulo  $L$ ", i.e., multiples of  $L$  were ignored:  $x=1.25L$  was identified with  $x=0.25L$ , for instance.

At each instant the accelerations of 512 charge disks due to the remaining 511 were thus computed and the record of displacements built up step by step. The time interval was  $\frac{1}{4}\omega_{pe}^{-1}$ , or about one twenty-fifth of a plasma period. A higher difference correction formula was used in the integration of the motion. (A non-growing mode at one-half of the plasma period can be found from the dispersion formula (1), and steps should be small enough to cope with this mode.)

The time unit employed for records was  $\omega_{pe}^{-1}$ , or  $1/2\pi$  of a plasma period (see Figs. 5 and 6), the space unit was  $L$ . The only other parameters in Eqs. (34) are the applied field in certain units and the mass ratio  $M/m$ . The field was taken zero. For the mass ratio the value for hydrogen was chosen. Apart from this specialization, the calculation is fully representative of all conditions. However, one should keep in mind that the restriction to one-dimensionality represents a considerable specialization.

Since the linear theory is sound up to the level of overtaking (see Sec. IX), initial perturbations were fed into the computation at a fairly high level, with electron displacement amplitude  $\frac{1}{3}L$ , just short of overtaking which occurs at  $L/2\pi$ . The ratio of ion and electron amplitudes is the same for displacements as for densities and hence given by (30). That of velocities is given by (29). Initial data were set up accordingly. There are phase differences also: relative to the electron displacements one finds  $+\pi/3$  for the ion displacements,  $+\pi/2$  for the electron velocities,  $+\pi/6$  for the ion velocities.

Accuracy or realism in the initial data are not essential: in a self-amplifying process the unfavorable modes excited initially will soon be overshadowed by the growing modes selected in the process. Ideally one would start the computation from its own internal noise, i.e., the random errors, and build up the fluctuation into the nonlinear regime automatically. However, computing time was costly and a start was made from a high-level input. The first few steps could be checked against the linear theory and were found to agree, thus reducing the chance of a mistake in the computing procedure to the unlikely coincidence between such a mistake and possible errors due to linearization of the analysis.

Since the input amplitude was  $\pi/4$  of the critical amplitude calculated at the end of Sec. IX, the fluctu-

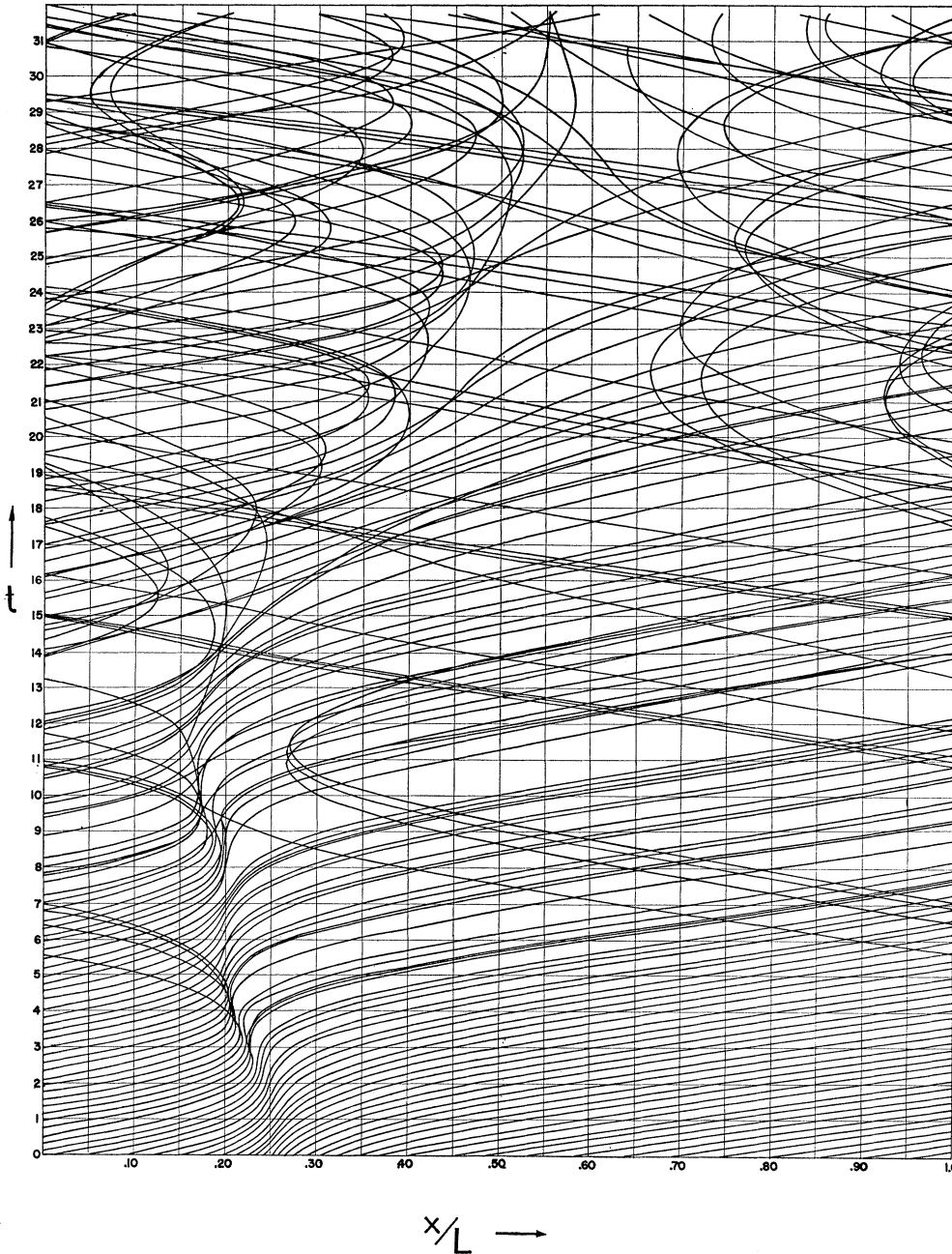


FIG. 5. Time-displacement graphs of 32 electron sheets (out of 256 computed).  $t$ , in units of  $\omega_{pe}^{-1}$ , versus  $x$  in units of  $L$ . Initial condensation as given by linear theory.

ation energy at input was already 62% of the initial drift energy which leads, through linear buildup, to the establishment of the wavelength  $L$  [drift velocity  $\omega_{pe}L/2\pi$ , see (5d)]. Only 38% of the initial drift energy should have been left, giving 62% of the initial drift velocity. Unfortunately, this point was overlooked and the electrons injected at the full initial drift velocity, plus fluctuations. The calculations therefore imply a booster field which has imparted the missing energy to

them. Since the main object of the calculations is to demonstrate the ability of fluctuations to destroy (and even reverse) the initial drift, we have erred on the right side.

Perhaps a more serious error which has crept into the calculations is the omission of the "self force" of each disk. The instruction given for the evaluation of the accelerations from Eq. (34) was to count the electron and ion disks *to the left* of the disk to be accelerated, not

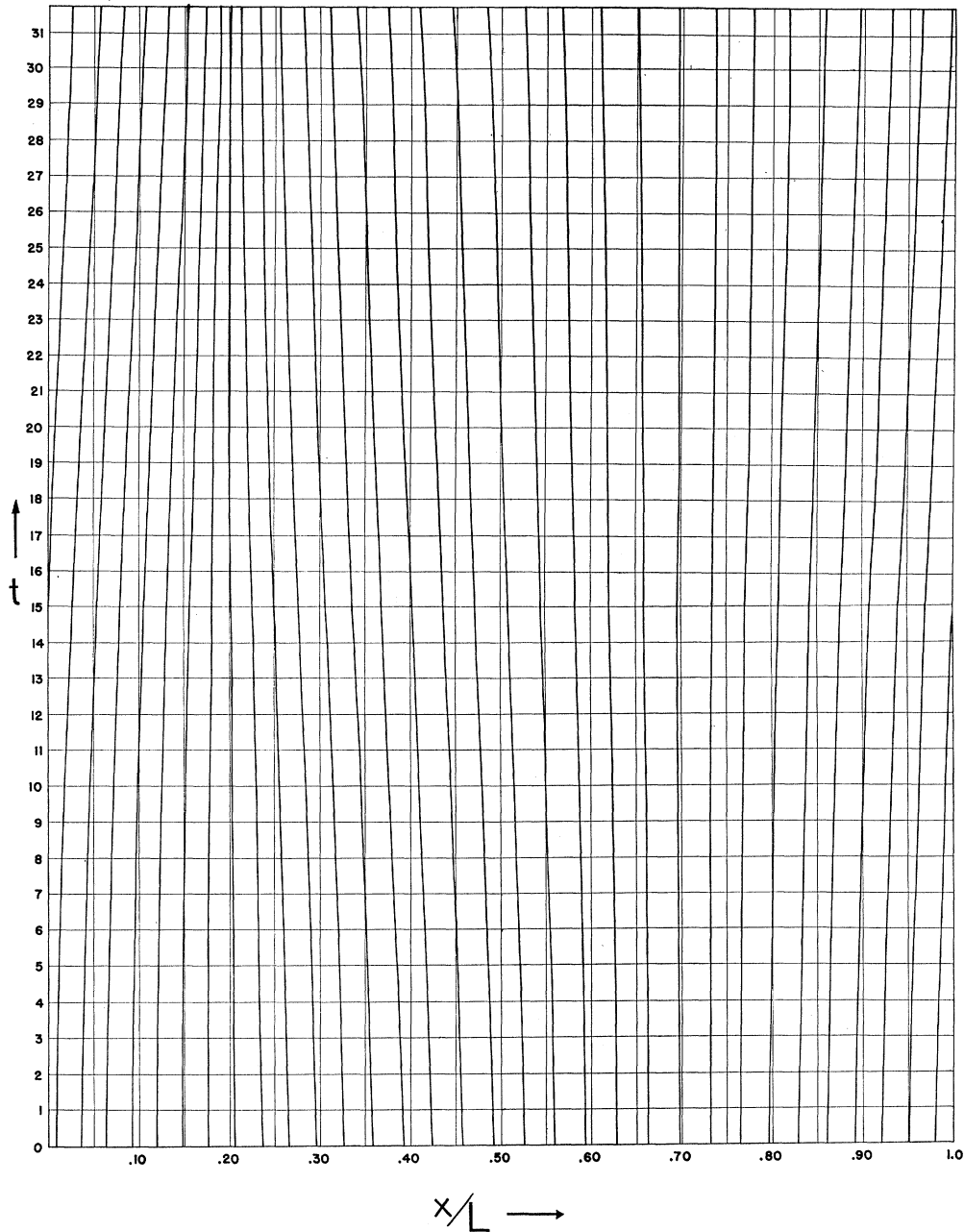


FIG. 6. Time-displacement graphs of 32 ion sheets (out of 256 computed). Scales as for Fig. 5.

including the disk itself. It would have been more correct to count the disk itself as one half of a disk. With a sufficient number of sufficiently thin disks ( $\delta s$  sufficiently small), this "self-force" becomes negligible.

However, in the actual calculations, with  $\delta s = L/256$ , the omission of the self-force had significant effects over the time interval (five plasma periods) for which the calculations were run. As a result, the ion and electron momenta would not balance. The appropriate correction due to the self-force was inserted and then the momen-

tum balance was found to be restored exactly, giving a good check of the numerical procedure. Broadly speaking, the self-force would not introduce any qualitative change of the numerical results obtained, but it would introduce a general delay of the phenomena by about one plasma period over the five plasma periods of the completed run.

Equations (34) and the initial conditions were programmed by Mr. D. Thoe of the Lockheed M.S.D. Computer Service into their 1103 AF digital machine

which then completed the calculations in approximately two hours. A record of the displacements of every eighth electron and every eighth ion was printed out by the machine, together with records of  $\bar{x}_e$  and  $\bar{x}_i$ . The rates of change of the latter quantities give the electron and ion currents.

#### XI. TRANSITION TO MULTISTREAM MOTION

The displacements of 32 electrons (out of 256 calculated but not recorded) were plotted as time-displacement graphs by J. Seger of Electronics Research Laboratories, Stanford. These plots are shown in Fig. 5. The displacements of 32 ions (out of 256 calculated) were also plotted and are shown in Fig. 6. When studying these graphs one should keep in mind the spatial periodicity: the left and right borders of the diagram join continuously and some electrons can be seen to sweep across the diagram several times.

The first impression given by the electron diagram (Fig. 5) is one of transition from order to chaos. To begin with (bottom of diagram) the electrons keep their original order and the initial condensation at  $x = \frac{1}{4}L$  intensifies, as predicted by linear theory. At  $t = 3\omega_{pe}^{-1}$ , overtaking occurs for the first time. Electron layers hesitate and build up a wall of space charge from which subsequent electrons are reflected, showing directly how "collective collisions" take place. Note, however, that the electrons bounce off their own fluctuation fields while the ions are still almost uniformly spaced. So far, the function of the ions has only been to *excite* the electron fluctuations.

The first electron wall disperses for a short interval, then intensifies again and causes further reflections. Some electrons which have already suffered one reflection bounce off again, from the other side of the wall and are "trapped" between adjacent walls. Others have sufficient energy to penetrate all walls, some in the forward and some in the reverse direction. The total electron current, obtained from the rate of change of  $\bar{x}_e$  (recorded), decreases steadily and reverses at about  $t = 30\omega_{pe}^{-1}$ , allowing for the self-force error. A very small ion current is set up. The main electron wall shifts in phase and eventually it is the rarefaction of the ions (at  $x = 0.7L$ , see Fig. 6) which repels electrons, while their concentration (at  $x = 0.2L$ , Fig. 6) traps them. There is an obvious tendency towards neutrality, and the material forms layers, a distance  $L$  apart.

The first occurrence of overtaking indicates the breakup of single stream motion into double stream motion. From then on, two electron disks are present at the same location in some range of the basic interval, and the two disks move with different velocities. Such a breakup occurs again and again until eventually (at  $t = 31\omega_{pe}^{-1}$ ,  $x = 0.55L$ ) about five different streams seem to interpenetrate.

When studying Fig. 5 it should be remembered that the curves do not represent trajectories of individual

electrons but that they represent a few selected electron sheets each of which stands for eight sheets or disks actually traced numerically, and each of those traced stands for a section of a continuum. In some places the continuity between adjacent sheets is still apparent at the top of the diagram, in spite of the omission of seven intermediate sheets from illustration. However, the continuum must have been "torn" a great many times and one-time neighbors become widely separated, to lead to the chaotic appearance of the top of Fig. 5. The order in which the 32 illustrated sheets are found at the top is this: 13, 24, 1, 19, 11, 12, 9, 6, 3, 18, 14, 32, 22, 16, 29, 23, 30, 28, 15, 20, 26, 31, 10, 4, 27, 8, 7, 17, 25, 5, 2, 21. Certain pairs, such as (11, 12) and (7, 8) have stuck close together. Others can still be identified as forming a coherent stream, such as (22, 23), (24, 25) and the triplet (29, 30, 31). The streams in these three cases are rather tenuous. Plots of the intermediate seven trajectories would be needed in order to recognize all of the orbits plotted in Fig. 5 as members of coherent streams rather than individuals. Perhaps even then there would be some strays, but on the whole one has the feeling that at the end of the run the computing machine was still handling coherent streams as families of *several* sheets rather than by one representative member only. It was therefore getting a fairly true picture of the charge distribution from which it calculated the field.

Up to the end of the run no crossing-over had occurred among the ions (see Fig. 6). However, there is convergence of ion trajectories at the condensation. This is not necessarily inhibited by ionic space-charge repulsion since we observe the trapping of electrons into these condensations. One would therefore expect a "clash" of ions to develop before many more plasma periods have elapsed. The mutual velocity of two interpenetrating streams of ions should greatly enhance the probability of a nuclear reaction in an individual encounter and a controversy will be released whether this should be classed as a "thermo"-nuclear phenomenon.

#### XII. "TURBULENCE" AND FURTHER RANDOMIZATION

The breakup of ordered motion into more and more complicated flow patterns, and the distribution of initial directed energy into more and more degrees of freedom by subdivision of the continuum suggest a comparison with hydrodynamic turbulence. The only forces taken into account are inertia and "Coulomb" pressure. There is no viscosity when one works on our scale, because of the rarity of individual particle collisions.

However, the "turbulence" illustrated in the top of Fig. 5 (one might refer to it as "electrodynamic turbulence") differs from hydrodynamic turbulence in the following respects: (a) it is one-dimensional, (b) the fluid can interpenetrate itself. In hydrodynamics one

cannot get one-dimensional turbulence *because* the fluid cannot interpenetrate itself. Two-dimensional motion (eddy formation) is therefore bound up with hydrodynamic turbulence.

The analog to the hydrodynamical dissipation of energy by turbulence, through the formation of smaller and smaller eddies, is to be seen in the redistribution of directed energy into the motions of increasing numbers of increasingly tenuous streams. Successive streams carry fewer and fewer particles: eventually the energy is distributed among individual particles and we have raised the temperature of the plasma. (The *initial* temperature implied in the calculations might be identified with the rounding-off errors: no spread was added artificially to the "cold" starting conditions of ions at rest and electrons in uniform motion.)

Long before such a complete dispersal of the energy into equipartition between all the microscopic degrees of freedom, a form of velocity distribution is reached which resembles the Maxwellian distribution. Everywhere there are superimposed many streams at different velocities and the "hot spot" at  $t \approx 31\omega_{pe}^{-1}$ ,  $x \approx 0.55L$  in Fig. 5 provides an example of this state of affairs. Indeed, one could scan the entire width in  $x$  at that time  $t$  to find the number of superimposed streams at each  $x$ , as well as the first two moments of their velocity distributions (local drift and local "temperature"). This description of the chaos suggests a statistical method of integrating further (for the electrons, not the ions). Unfortunately, the equations for the moments of the distributions do not "close" without some assumption about the rate of heating; the integration of the full dynamical equations eliminated the necessity for a guess about the rate of heating.

Throughout this calculation single collisions between individual particles have been ignored. The randomization of energy is entirely due to collective Coulomb interaction. If one had to wait for collisions, the time scale for randomization would be stretched by a very large factor.

The use of thermodynamical terms in situations which are a long way from statistical equilibrium usually meets with criticism. To side-step the controversy, we might avoid the word "temperature" by talking only of the mean mutual velocity of interpenetrating streams. When it comes to interpenetration of ion streams (extrapolation of Fig. 6), it is this mutual velocity which determines nuclear reaction rates. At that stage, there are present only a few well-formed streams or "beams," interpenetrating each other like a cyclotron beam and its target. This state of affairs arises long before strict thermal equilibrium of all particles is created by individual collisions. If we are unwilling to broaden our thermodynamical terminology, we must accept the fact that a true "thermo"-nuclear regime will tend to be by-passed by "collective" Coulomb effects which get there first.

### XIII. GROWTH OF INSTABILITIES UNDER A STEADY APPLIED FIELD

Our work demonstrates the braking of electrons when coasting after acceleration by an electric pulse which does not itself create disorder. No violent instabilities should occur during a pulse shorter than, say, 10 plasma periods. For the "typical" example of Sec. III, this means a field of magnitude

$$(m/e)u/(20\pi\omega_{pe}^{-1}) = mu^2/10Le = 15 \text{ kilovolt/cm.}$$

This is not an excessive field to realize: the main problem would be how to shut it off after only 10 plasma periods (about  $3 \times 10^{-11}$  second at  $N = 10^{15} \text{ cm}^{-3}$ ).

We obviously require an analysis of the case where a field of more moderate strength continues to prevail, slowly increasing the mean drift while instabilities build up and eventually, perhaps, maintaining the drift against the dissipation in instabilities.

Since instabilities take times of the order  $\alpha_m^{-1}$  to develop (see Sec. II), it is reasonable to suppose that drift velocities measuring several times  $e|E|/m\alpha_m$  can be created by an external field  $E$  in moderately "pure" form (we omit the bar over  $E$  in this section: the applied field is meant throughout). Subsequently, the *relative* change of the drift velocity during an  $e$ -folding time of the amplitudes will be small and we may apply an "adiabatic" theory.

According to Sec. II, the wave numbers  $\beta$  in an interval of width  $\frac{1}{4}\omega_{pe}/u$  around the value  $\omega_{pe}/u$  are amplified strongly. As for our rougher estimate at the beginning of Sec. VI, we shall take the growth rate to be  $\alpha_m$  in this interval and zero outside, replacing the actual dispersion curve by a "square top" function (see Fig. 1). Amplification of a particular wave number lasts only while  $u$  is within a band of width  $\frac{1}{4}\omega_{pe}/\beta$  around the value  $\omega_{pe}/\beta$ . At other times, we might say, that wave number is "out of resonance." The duration of amplification is therefore limited to  $\frac{1}{4}m\omega_{pe}/e|E|\beta$  and fluctuation energy amplified only by a factor  $\exp(\tau)$  where

$$\tau = 2\alpha_m \times \text{duration} = \frac{1}{2}m\omega_{pe}\alpha_m/e|E|\beta. \quad (41)$$

While in Sec. VI we had unlimited amplification of a narrow band of  $\beta$ -values, we now get limited amplification of an unlimited range of  $\beta$ -values. At time  $t$  the  $\beta$ -values in the vicinity of  $m\omega_{pe}/e|E|t$  are unstable. Short waves (large  $\beta$ ) become unstable first and at time  $t = t_1$  all  $\beta$  down to about  $m\omega_{pe}/e|E|t_1$  will have undergone amplification. Hence a maximum exponent  $\tau$ , to be denoted  $\tau_1$  and equaling  $\frac{1}{2}\alpha_m t_1$ , can be achieved with the latest, and longest, wavelengths: these contribute the largest amount of amplified fluctuation energy.

It is not important to fix an accurate lower limit to the wavelengths contributing to amplification. The Debye length sets one lower limit, but often a more severe limitation arises from the condition that our "adiabatic" theory should apply, namely that the mean velocity during amplification,  $\omega_{pe}/\beta$ , should exceed

its change during an  $e$ -folding time of amplitude  $e|E|/m\alpha_m$ . It means the  $\beta$ -values must be small enough, and the wavelengths long enough, to make the exponent  $\tau$  in (41) of the order unity at least. We shall, therefore, integrate over that wavenumber band which makes the exponent  $\tau$  run from 1 to  $\tau_1$ .

The initial fluctuation energy contained in a wave-number band  $\delta\beta$  was found in the last paragraph of Sec. V to be  $(\delta\beta/18)kT/(2\pi\lambda_D)^2$  per unit plasma volume. The fluctuation energy per electron is therefore  $\delta\beta e^2/18\pi$ , after substitution for  $\lambda_D$  from (5c). We now use (41) to get  $\delta\beta$  in terms of  $\delta\tau$ ,

$$\delta\beta = -\frac{1}{2}m\omega_{pe}\alpha_m\delta\tau/\tau^2 e|E|, \quad (42)$$

and on integrating over our range of  $\tau$  we obtain

$$\begin{aligned} &\text{fluctuation energy} \\ &= (e^2m\omega_{pe}\alpha_m/36\pi e|E|) \int_1^{\tau_1} \exp(\tau)d\tau/\tau^2. \end{aligned} \quad (43)$$

For large  $\tau_1$  the integral is approximately  $\exp(\tau_1)/\tau_1^2$  and insensitive to the lower limit. For  $\alpha_m$  we use the hydrogen value  $0.0562\omega_{pe}$  (all these calculations are for hydrogen). Then we substitute for  $\omega_{pe}^2$  from its definition,  $4\pi N e^2/m$ . We use  $W = e^2/l$  as reference energy [see (6)] and define a corresponding reference field,  $E_0$ , as follows:

$$\begin{aligned} E_0 &= e/l^2 = 1.44 \times 10^{-7} l^{-2} \text{ volt cm,} \\ &\text{Coulomb field experienced by closest} \\ &\text{neighbor in cubic lattice.} \end{aligned} \quad (44)$$

This reference field is proportional to  $N^{2/3}$  and at  $N = 10^{15}$  per cc its value is 1.44 kilovolt per cm. With all these substitutions, we get the fluctuation energy per electron at the time  $t_1 = 2\tau_1/\alpha_m$  in the form:

$$\begin{aligned} &\text{fluctuation energy} \\ &= (1/160)W|E_0/E| \exp(\tau_1)/\tau_1^2. \end{aligned} \quad (45)$$

At the same time  $t_1$  the drift energy will have been built up to

$$\begin{aligned} \text{drift energy} &= \frac{1}{2}(eEt_1)^2/m = 2e^2E^2\tau_1^2/m\alpha_m^2 \\ &= 2 \times 0.0562^{-2} e^2 E^2 \tau_1^2 / m\omega_{pe}^2 \\ &= 50W|E/E_0|^2 \tau_1^2, \end{aligned} \quad (46)$$

after substitution from the definitions of  $\omega_{pe}$ ,  $W$ , and  $E_0$ . The fluctuations will always catch up with the drift eventually, namely when the expressions on the right of (45) and (46) become equal:

$$|20E/E_0|^3 \tau_1^4 = \exp(\tau_1). \quad (47)$$

Roughly,  $\tau_1$  goes up like  $3 \ln |E/0.05E_0|$ . The comparison field  $0.05E_0$  in this estimate is quite small, only 72 volts per cm at  $N = 10^{15} \text{ cm}^{-3}$ . Since  $\tau_1$  measures time in multiples of 5.67 plasma periods, a field whose strength is measured in kilovolts per cm would be able to increase the drift unhindered for as many as 100 plasma periods. At 30 plasma periods the value of

$|E/E_0|$  determined from (47) is 0.03, at 100 plasma periods it is 0.4, but at 170 plasma periods it is 11.8. The time over which drifts can be built up is therefore of the order of 100 plasma periods for a wide range of applied fields.

#### XIV. "RUNAWAY"

The estimates of the times during which acceleration can take place unhindered must be modified for very weak fields, for several reasons. First, the approximation following Eq. (43) becomes poor when  $\tau_1 < 5$  ( $t_1$  less than 30 plasma periods). But it would still be true to say that less than 30 plasma periods suffice to destroy drifts created by fields weaker than  $0.03E_0$  if it weren't for the remaining reasons.

Second, Landau damping stabilizes the shorter wavelengths, or, as shown in Sec. IV, instabilities do not set in till the drift energy exceeds  $0.9kT$ . A field will create stable drifts of this magnitude but provoke instabilities when accelerating the electrons further. The time for accelerating to  $0.9kT$  energy is  $0.43(2\pi\lambda_D/l)(E_0/E)$  plasma periods, using formulas (5) and (44). For the lowest fields mentioned above and the typical proportion (8), this amounts to several hundred periods against which the time for the subsequent development of instabilities is rather insignificant. For large fields the significance is reversed.

Third, weak fields may take more than one collision interval to accelerate electrons to  $0.9kT$ . The mean free path at velocity  $u = (2kT/m)^{1/2}$  can be obtained from (9) by substituting  $L = 2^{3/2}\pi\lambda_D$ , in accordance with (7). One obtains  $16\pi\lambda_D^4 N$ , or  $(2\lambda_D)^2 kT/e^2$  after using (5c). We multiply by  $e|E|$  to get the energy gained from the field between collisions. This should exceed  $kT$  (roughly) and hence:

$$|E| > e/(2\lambda_D)^2 = \text{Coulomb field at distance } 2\lambda_D. \quad (48)$$

For the "typical" example in Sec. III one gets 15 volts/cm.

Electrons which have been accelerated to energies exceeding  $kT$  before making a collision will continue to be accelerated without hindrance since their collision cross section rapidly decreases as they get faster. These are termed "runaway" electrons.<sup>8-10</sup> They have nothing to do with classical "runaway" electrons of Dirac<sup>11</sup> which are accelerated by their own radiation field. In the sense that the present analysis deals with electrons unhampered by collisions, it might be called an analysis of "runaway" conditions.

The field given by (48) is, in fact, a "runaway" field. It is quite low and decreases with temperature, being proportional to  $N/T$ . There must be many conditions

<sup>8</sup> C. T. R. Wilson Proc Cambridge Phil. Soc. 22, 534 (1925).

<sup>9</sup> A. S. Eddington, *The Internal Constitution of the Stars* (Cambridge University Press, Cambridge, 1926), pp. 302, 320.

<sup>10</sup> F. Hoyle, *Some Recent Researches on Solar Physics* (Cambridge University Press, Cambridge, 1949).

<sup>11</sup> P. A. M. Dirac, Proc. Roy. Soc. London A167, 148 (1938).

where fields of this magnitude are applied to plasmas and where the electrons ought to run away. In fact, we have shown that electrons do *not* run away indefinitely. Their acceleration will be braked by instabilities after some 100 plasma periods. We might say that collisions in bulk then take over from the close collisions which the "runaway" electrons have escaped.

There is, however, a form of runaway that might persist for a long time and lead to high velocities. A small number of fast electrons in the Maxwellian tail of the initial distribution, or, more likely, some tenuous streams such as those seen streaking across Fig. 5 in either direction as a result of the instabilities, can proceed as a separate group, unhindered both by collisions and by the space-charge forces in the bunches, their velocity being too high. By the two-stream mechanism, they might interact with the ions and the bulk of the slow electrons. But since they are few in number their plasma frequency is low and instabilities will build up among them only slowly. They will enjoy free acceleration by the applied field for a long time and gain higher and higher energies.

#### XV. ELECTRODYNAMIC HEATING AND RESISTIVITY

In Sec. XII we discussed the conversion of drift energy into the random energy of many superimposed streams. While we envisaged eventual equipartition of the initial drift energy into a random distribution of velocities of individual particles, we were unable to suggest a time scale, other than the very long time scale based on the mechanism of close collisions, for this process. We also discussed the merits of applying thermodynamical terms to such pre-equilibrium velocity distributions as are shown at the top of Fig. 5.

A terminology is justified by its uses and for the purposes of the ensuing arguments it does not matter whether a certain velocity distribution is completely random and equipartitioned down to individual particles, or whether there is a good deal of coherence, or "streaming in bulk." We shall therefore speak freely of "heat" in connection with the pre-equilibrium distribution and ascribe a temperature to it.

The new temperature  $T'$  created by the instabilities is defined as the mean energy of a streaming electron, divided by  $k$ . The energy has come out of the initial drift and hence  $kT'$  will be of the order  $\frac{1}{2}mv^2$ . It will

have risen to this value from the initial  $kT$  and in this sense we have "heated" the plasma without collisions, purely electrostatically.

In Sec. IV we found the extent to which instabilities are suppressed by Landau damping and the argument here was based on the superposition of many streams of electrons of different velocities, their mean kinetic energy being  $\frac{1}{2}kT$ . Equipartition down to individual electrons was not implied. The calculations were done for a strict Maxwellian distribution, but similar results are obtained with other types of distribution. (We refrain from reproducing such calculations here: in many cases they are easier than for the Maxwellian distribution.)

Once the new distribution is established at temperature  $T'$ , we may conclude that drifts of the order  $kT'$  are required to be produced by a sustained electric field before instabilities develop again, on a new level, giving further heating and raising the temperature to  $2kT'$ , etc. Only very few plasma periods seem necessary for a disordering of streams after the fluctuation energy has caught up with the stream energy.

We now get the following picture of the dissipation of energy, and of the "electrodynamic heating" of a plasma: a strong field creates a drift for something like a hundred plasma periods. After this the drift is randomized and turned into heat. The drift can now build up again, but as soon as it reaches the energy corresponding to the new "temperature," instabilities are set up again. The temperature is thus driven up and up by the electric field and a drift exceeding the random energy never persists for long: the temperature adjusts itself to inhibit instabilities but as soon as the field pulls the electrons away, instabilities raise the temperature.

Since a field can accelerate for something like a hundred plasma periods, the drift velocity is of the order  $200\pi e|E|/m\omega_{pe}$  and the current density has  $eN$  times this value. The conductivity is therefore  $200\pi e^2N/m\omega_{pe} = 50\omega_{pe}$  in electrostatic units. In mks units this becomes  $200\pi\epsilon_0\omega_{pe}$  which is a factor  $20\pi$  larger than estimated rather crudely in reference 1, but still very small compared with the conductivity based on close collisions.

We conclude that fields in excess of the runaway value (48) create currents which are dissipated in instabilities. This provides a resistivity much larger than that due to individual collisions: collisions in bulk take over.